Lift Force and Dynamical Unbinding of Adhering Vesicles under Shear Flow

Isabelle Cantat and Chaouqi Misbah
Laboratoire de Spectrométrie Physique, Université Joseph Fourier (CNRS), Grenoble I,
B.P. 87, Saint-Martin d'Hères, 38402 Cedex, France

(Received 21 January 1999)

We show that a vesicle under shear flow experiences a lift force of hydrodynamical origin. This force is of purely viscous nature, and it originates from upstream-downstream asymmetry. At a critical shear rate $\gamma \simeq 100-500$ Hz the vesicle, initially making adhesion with a substrate, undergoes an unbinding transition in two nontrivial steps. In the first step the lift force behaves as γ^2, whereas in the second step as γ. We present numerical and analytical results on this phenomenon. We discuss several implications.

PACS numbers: 87.16.−b, 47.55.Dz, 87.19.−j

A long time ago Lord Rayleigh reported that a spinning ball experiences a lateral force and has credited this phenomenon to Magnus. Poiseuille [1] in 1836 recognized that blood corpuscles in the capillaries tend to keep away from the walls due to a *lift force*. These two forces are of different natures, the latter stems from viscous effects, while the former originates from inertia. In the realm of cell biology, inertia is small (the Reynolds number is at most equal to 10^{-3}), and thus viscous effects prevail. A lift force of viscous type cannot act on a spherical object owing to the reversibility of the hydrodynamics equations in this limit (Stokes equations). However, vesicles are deformed during motion, as, for example, under shear flow. Their form has upstream-downstream asymmetry which destroys reversibility upon time reversal. This results in a lift force of purely viscous nature. It is several orders of magnitude larger than the usual Magnus force [2]. Determining this force, and analyzing its far reaching consequences, is the first goal of this Letter.

The analysis is performed on phospholipidic vesicles. The vesicle form is not given *a priori*; it adapts its shape freely to the environment (a free boundary problem). The problem is nonlinear and nonlocal (see below). We find that the vesicle, initially making adhesion with a wall, detaches completely from the wall when the shear rate γ exceeds a critical value. This scenario occurs in two distinct nontrivial steps and it results from a subtle interplay between lift force, bending, and adhesion forces. For typical parameter values of phospholipidic vesicles, the critical shear rate falls in the range of 100 s^{-1}. Using a lubrication approximation we extract analytically the functional dependence of the lift force. We provide also an expression for the *dynamical contact curvature* when the vesicle still adheres to the substrate. The analytical work is supported by the full numerical analysis.

The vesicle initially makes adhesion with a homogeneous substratum and is submitted to a constant linear shear flow. In the limit of a small Reynolds number the velocity field obeys the Stokes equations, which are linear. The superposition theorem implies that at any point in the fluid the velocity is the sum of two terms: (i) the velocity of the unperturbed shear flow $\mathbf{v} = \gamma y \hat{\mathbf{x}}$ (in the coordinates system shown in Fig. 1), with γ the constant velocity derivative along the y direction; (ii) the velocity response to the forces applied on the fluid by the vesicle and the substrate. This term is written by using a Green's function formalism, with $\overline{\overline{T}}$ the free space Green's tensor [3]. Considering a 2D situation, which is sufficient in order to capture all of the features, we obtain

$$\begin{aligned}\mathbf{v}(\mathbf{r},t) = &\int_{\mathrm{memb}} \overline{\overline{T}} \cdot \mathbf{f}'_{\mathrm{memb}}\, ds' \\ &+ \int_{\mathrm{subs}} \overline{\overline{T}} \cdot \left(-\eta \frac{\partial \mathbf{v}'}{\partial y'} + p'\hat{\mathbf{y}}\right) dx' \\ &+ \gamma y \hat{\mathbf{x}}\,.\end{aligned}$$

The membrane force $\mathbf{f}_{\mathrm{memb}}$ is obtained as a functional derivative of the Helfrich free energy supplemented with the adhesion potential w,

$$\begin{aligned}\mathbf{f}_{\mathrm{memb}} &= -\frac{\delta F}{\delta \mathbf{r}} = -\frac{\delta}{\delta \mathbf{r}} \int ds \left[\frac{\kappa}{2} c^2 + \zeta + w[\mathbf{r}(s)]\right], \\ &= \left[\kappa\left(\frac{\partial^2 c}{\partial s^2} + \frac{c^3}{2}\right) - c\zeta\right]\mathbf{n} - \frac{\partial w(y)}{\partial y}\hat{\mathbf{y}} + \frac{\partial \zeta}{\partial s}\mathbf{t}\,,\end{aligned} \tag{1}$$

where ζ is a Lagrange multiplier enforcing a constant length (whereas the enclosed volume conservation is ensured by fluid incompressibility), $\mathbf{n}$ and $\mathbf{t}$ are the normal and tangent unit vectors, $\kappa \sim 25kT$ is the bending rigidity, and c is the curvature. The adhesion potential has a minimum denoted by $w_0 \sim 10^2 kT\ \mu\mathrm{m}^{-2}$ at a distance from the substrate $d_0 \sim 50$ nm.

A description of the numerical strategy is given in [3,4]. After the transient has decayed, the vesicle moves in a shape-preserving manner with constant velocity. On increasing γ, the vesicle undergoes series of transformations before it reaches the unbinding threshold, as shown in Fig. 1. Three typical behaviors are revealed on increasing shear rate.

© 1999 The American Physical Society

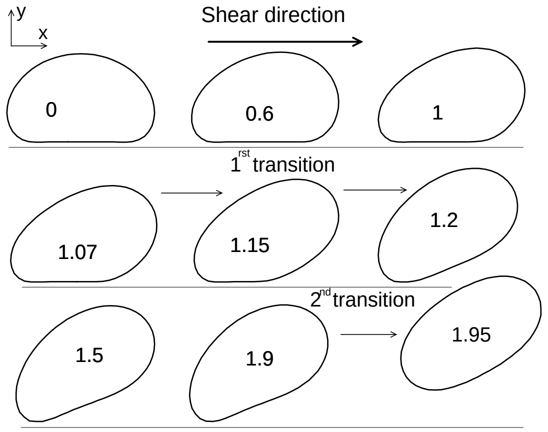

FIG. 1. Stationary vesicle shape evolution under an increasing shear rate. (The numbers refer to typical shear rate values measured in units of 100 s^{-1}.)

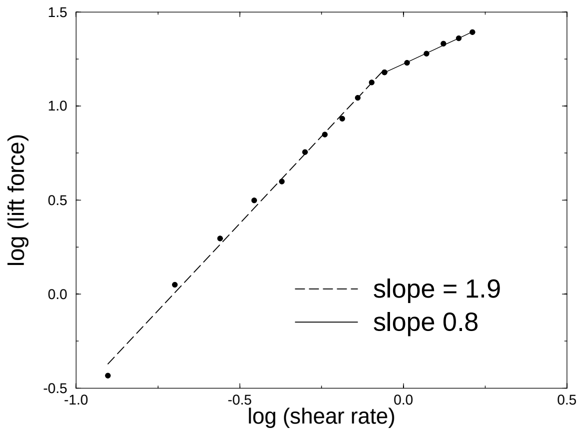

FIG. 2. Hydrodynamical lift force as a function of the shear rate in logarithmic scales.

Small shear rate.—The vesicle still strongly adheres to the substrate (first three states in Fig. 1). The front part of the vesicle moves upward progressively, whereas the rear develops a stronger contact curvature with the substrate.

Intermediate shear rate.—For a critical value of the shear rate γ_1 the surface of adhesion (length in 2D) undergoes a *sudden* (within few percent change of γ) collapse towards zero; the vesicle remains only pinned to the substratum. An important feature is that the vesicle morphology then remains practically unchanged over a wide range of the shear rate (typically a factor of 2). The only noticeable evolution is the increase of the tank-treading and translational velocities. The tilt and shape of this pinned vesicle are close to those of a vesicle in an unbounded shear flow which only depends on the reduced volume of the vesicle, and not on the shear rate [5].

Large shear rate.—The vesicle completely unbinds at a second critical shear rate $\gamma_2 \sim 100\ s^{-1}$ (for typical parameters used before, and for a vesicle radius of order 10 μm) and is pushed away from the wall.

The decomposition of the unbinding transition into two separate processes is fully justified by the lift force evolution as a function of the shear rate (Fig. 2). The numerical power law exhibits clearly a slope discontinuity. The first exponent 1.9 is valid on a whole decade and remains constant ±5% for different rigidity or adhesion values. The second exponent is obviously not so precise because of the limited range of shear rate values between the first and second transitions. It can practically be assigned a value of about 0.8. Under a small shear rate, the vesicle behaves as a deformable object and a dimensional analysis predicts a quadratic law with γ [6]. As we have seen, for larger shear rates the shape does not evolve noticeably, so the law must be linear.

The asymmetry of the pressure field produces a torque which is responsible for the first transition (see Fig. 3). This happens as soon as the attractive potential cannot counterbalance the overpressure *locally* in the front part (at the rear there is an underpressure entailing an enhancement of the binding to substrate). The whole vesicle tilts to assume the *most favorable shape*. The second transition takes place when the *total* lift force overcomes the adhesive force. These features are discussed below.

As stated before, the viscous lift force vanishes for a symmetrical object. This fact is traced back to the reversibility of the Stokes equations. Thus, the first concern will focus on the estimate of the shape asymmetry. Both adhesion and hydrodynamical forces are only important in the vicinity of the substrate and, especially, close to the vesicle contact points. In order to quantify the shape asymmetry in this region, we compare the curvature at the front and rear contact points. The determination of these curvatures is very interesting by itself. It provides us with a central result, that is, *dynamical contact curvature*.

The flow produces an overpressure in front of the vesicle and an underpressure in the rear (see Fig. 3). Using the Landau-Levich lubrication approximations in the region of interest between the substrate and the

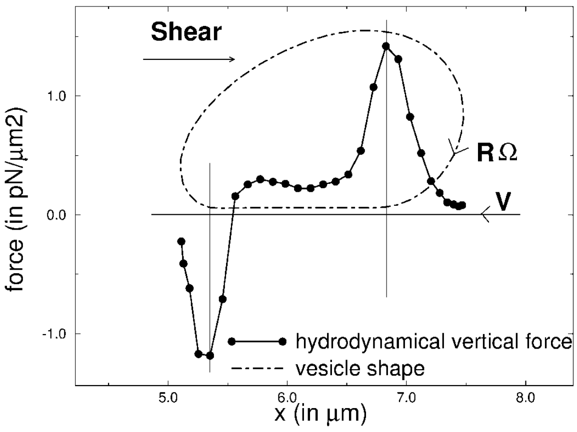

FIG. 3. Hydrodynamics vertical force distribution under the vesicle. The forces exerted on the top are 1 order of magnitude smaller.

membrane, whose width is denoted as $d(x)$ (Fig. 4) the Stokes equations takes the form

$$\frac{\partial^2 v_x}{\partial y^2}(x,y) = \frac{1}{\eta}\frac{dp}{dx}(x), \qquad \frac{\partial v_x}{\partial x}(x,y) = -\frac{\partial v_y}{\partial y}(x,y). \tag{2}$$

The vesicle has a stationary motion with translational and tank-treading velocities denoted by $V\hat{\mathbf{x}}$ and $-R\Omega\mathbf{t}$, respectively. R is a typical vesicle radius, and $-\Omega$ is the rotation rate. In the vesicle frame moving at constant velocity $V\hat{\mathbf{x}}$, the boundary conditions are $\mathbf{v}(x,0) = -V\hat{\mathbf{x}}$ and $\mathbf{v}(x,d) = -R\Omega\mathbf{t}$. The vector $\mathbf{t} \simeq \hat{\mathbf{x}} + d'\hat{\mathbf{y}}$ is the unit tangent, and d' designates derivative of d. Using Eq. (2), we express v_x as a function of the pressure,

$$v_x(x,y) = \frac{1}{\eta}\frac{dp}{dx}\left(\frac{y^2}{2} - \frac{yd}{2}\right) + \frac{y}{d}(V - R\Omega) - V. \tag{3}$$

We choose an exponential profile [8] for both sides of the vesicle in the vicinity of the two contact points (Fig. 4), that is, $d(x) = d_0 e^{x/x_0^{\pm}}$; ± refers to the front and rear sides, and the origin for x corresponds to the contact point ($d = d_0$). Using the boundary conditions for v_y, we obtain a differential equation for the pressure. The integration is performed around each contact point with vanishing boundary conditions for the pressure at $d = d_0$ and $d \to \infty$. This is not fully true when compared to numerical values (Fig. 3), but provides a good approximation, and this is sufficient for our purposes. We obtain

$$p^{\pm}(x) = \frac{6\eta V_m x_0^{\pm}}{d^2}\left(1 - \frac{d_0}{d}\right), \tag{4}$$

where $V_m = (V + R\Omega)/2$ is the average velocity in the lubrication region measured in the translational vesicle frame. From the pressure field, we find that the extremal local pressure occurs for $d_m = \frac{3}{2} d_0$:

$$p^{\pm}_{\max} = \eta V_m \frac{x_0^{\pm}}{d_0^2}. \tag{5}$$

Note that x_0 is positive at the front and negative at the rear, meaning an overpressure ahead and an underpressure behind. The power laws are in good agreement with numerical results. The hydrodynamical force is proportional to the geometrical factor $x_0^{\pm}$. Realizing that dynamical curvature $c_d \sim d_0/(x_0^{\pm})^2$, we see that the total lift force depends on the curvature difference between the two contact points.

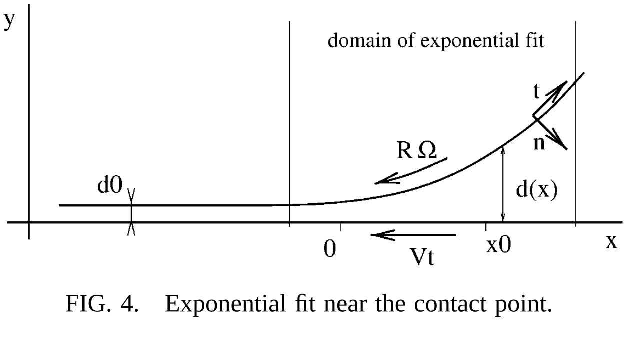

FIG. 4. Exponential fit near the contact point.

The interplay between the above lift force and adhesion and bending forces provides us with an equation for the curvature c_d. The distance d_0 plays the role of a small parameter (as compared to vesicle size). The two leading membrane forces in terms of d_0 are [Eq. (1)] $\kappa\partial^2 c/\partial s^2 \sim \kappa c_0/l_0^2$, and the adhesion force which varies rapidly close to the substrate is $\frac{\partial w}{\partial y} \sim w_0/d_0$. Here, l_0 is the characteristic distance of the curvature variation, and is practically independent of γ far from the first unbinding transition. For a contact adhesion potential the curvature jumps from zero on the substrate to its equilibrium value $c_0 = \sqrt{2w_0/\kappa}$ [7]. This obviously implies that $l_0 \to 0$ with d_0. In order for the curvature force to compensate the adhesive force, we must have, at equilibrium,

$$l_0 \sim \sqrt{\frac{\kappa c_0 d_0}{w_0}} \sim \sqrt{\frac{d_0}{c_0}}. \tag{6}$$

The hydrodynamical force also "diverges" for small d_0 [for a given V_m, see Eq. (5)]. It competes with the two dominant membrane forces presented above, and this is precisely how the *dynamical curvature* is obtained. Combining the three forces (hydrodynamics, bending, and adhesion) we arrive at

$$\begin{aligned} &\kappa\frac{c_d}{l_0^2} + \eta V_m \frac{x_0}{d_0^2} - \frac{w_0}{d_0} = 0, \\ &c_d - c_0 \sim \mp \frac{\eta\gamma\sqrt{R}}{\kappa^{1/4} w_0^{3/4}\sqrt{c_d/c_0}}. \end{aligned} \tag{7}$$

The minus and plus signs refer to the front and rear, respectively. We have used the fact that $V_m \sim V \sim \gamma\sqrt{Rd_0}$. This is the asymptotic result for a cylinder under shear flow moving along a wall for small d_0 [9]. Equation (7) is a third order equation for c_d. To leading order, $c_d/c_0 \sim O(1)$, so that dynamical deviations are linear in the shear rate. The dynamical curvature is decreased at the front and increased at the rear. This leads to an upward normal force directed toward the fluid, a lift force, as expected. At appreciable velocities, the third order equation is solved and compared to the full numerical solution for the forward curvature (upon scales adjustment). We find good agreement (Fig. 5). At the back part, the agreement is less satisfactory since, due to a curvature increase, nonlinear effects in the bending force [e.g., c^3 in Eq. (1)] act against the curvature increase and significantly limit the strength of variation. In other words, most of the effect is pronounced at the front part, whereas at the rear the curvature is within reasonable accuracy close to c_0.

Let us now determine the lift force together with the critical shear rate for the first transition. Transition occurs

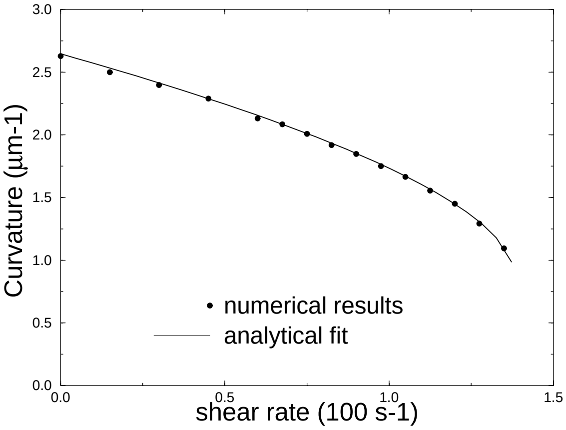

FIG. 5. Curvature evolution with the shear rate.

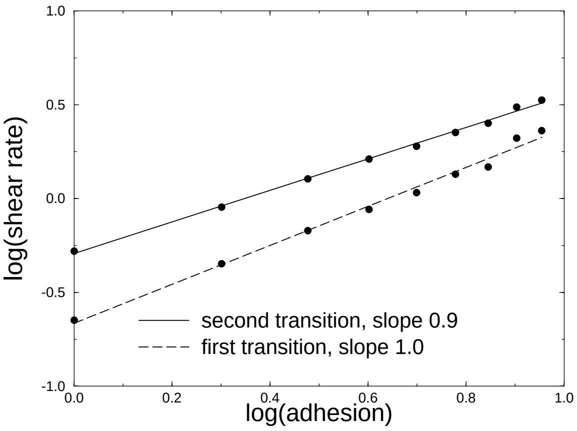

FIG. 6. Critical shear rate value for both transitions as a function of adhesion potential.

when the hydrodynamical force overcomes the adhesive force around the front part of the vesicle. The transition is characterized by a slope divergence in the curve $c_d(V_m)$. This entails that the critical shear rate be given by (see full numerics in Fig. 6)

$$\gamma_1 \sim \frac{w_0}{\eta}\sqrt{\frac{c_0}{R}} \sim \frac{w_0^{5/4}}{\eta\sqrt{R}\,\kappa^{1/4}}\,. \tag{8}$$

Under the assumption that the hydrodynamical force under the vesicle is $l_0 p_{\max}$, we determine the total lift force acting on the vesicle as $F_l = l_0[p_{\max}(c_d) - p_{\max}(c_0)]$,

$$F_l \sim \frac{\eta^2\gamma^2 R\kappa^{3/4}}{w_0^{7/4}\sqrt{d_0}}\,. \tag{9}$$

For larger shear rates, the shape asymmetry depends mainly on the vesicle tilt and the reduced volume. The shape is constant, independent of the rigidity and of the adhesion, so we do not need to estimate it in order to determine the total lift force evolution. We denote by $\bar{c}$ the mean curvature and by Δc the curvature difference between both sides of the (unique) contact point. Realizing that the force is mainly exerted on a length $l \sim \sqrt{d_0/\bar{c}}$, we obtain

$$F_{l2} \sim \eta V_m \frac{\Delta c}{d_0\bar{c}^2} \sim \eta\gamma\sqrt{\frac{R}{d_0}}\,\frac{\Delta c}{\bar{c}^2}\,. \tag{10}$$

The unbinding transition occurs when this force exceeds the adhesion force acting on the pinned portion. The latter is given by $w_0/\sqrt{d_0\bar{c}}$. This yields

$$\gamma_2 \sim \frac{w_0}{\eta}\sqrt{\frac{\bar{c}}{R}}\,\frac{\bar{c}}{\Delta c}\,, \tag{11}$$

where γ_2 is directly related to the vesicle asymmetry (the factor Δc). It depends linearly on the adhesion since at the unbinding threshold, the lift force does not vary as γ^2 but as γ instead. This result was not obvious *a priori*. It should provide an important basis for experimental investigations on cell adhesion.

Finally, let us make some general remarks. It is clear that the predictions made here are not devoid of experimental testability, and direct comparison with the present work can be made for vesicles making a weak adhesion with the substrate. For biological cells, or for vesicles decorated with specific adhesion centers, there exists a critical force above which a cell rolls under shear [6]. This effect can, in principle, be incorporated in our study by introducing adhesion pinning centers, or other effects that lead to a critical force. In the biological world, perhaps the most prominent example concerns leukocyte movement. The lift force tends to keep a leukocyte away from the venule wall. Venules of infected and inflamed tissue dilate and become leaky. This sufficiently perturbs the flow, thus allowing a leukocyte to reach the venule walls, where it can be caught by adhesion molecules. Similarly, due to a venule injury, elastic properties may also be significantly altered. The same should happen as one gets older. It is tempting to speculate that this should weaken the lift force, inducing thereby a deposit of some undesirable blood corpuscles on the venule wall. We hope that the present study will, in a concerted fashion with experimental analyses, shed light on the relevance of the results presented here to a wider variety of systems.

[1] J. L. M. Poiseuille, Ann. Sci. Nat. **5**, 111 (1836).
[2] P. Olla, J. Phys. II (France) **7**, 1533 (1997).
[3] I. Cantat and C. Misbah, Phys. Rev. Lett. **83**, 235 (1999).
[4] I. Cantat and C. Misbah, “Transport versus Structure in Biological and Chemical Systems,” edited by S. Müller *et al.* (Springer-Verlag, Berlin, to be published).
[5] M. Kraus, W. Wintz, U. Seifert, and R. Lipowsky, Phys. Rev. Lett. **77**, 3685 (1996).
[6] R. Bruinsma, in *Physics of Biomaterials, Fluctuations, Self Assembly and Evolution,* edited by T. Risk and D. Sherrington, NATO ASI Series E, Vol. 332 (Kluwer, Dodrecht, 1996).
[7] U. Seifert, Phys. Rev. A **43**, 6803 (1991).
[8] Because d is small, and the competing effects (curvature, tension, and hydrodynamics) are proportional to d with different derivatives, the simplest form is exponential.
[9] D. J. Jeffrey and Y. Onishi, Q. J. Mech. Appl. Math. **34**, 129 (1981).